Standardized Measures for the Stability Analysis of Low-Cost Digital Cameras and Potential Applications

Ayman HABIB, Anoop PULLIVELLI and Chang-Hahk HAHM, Canada

Key words: Photogrammetry, Digital Cameras, Calibration, Interior Orientation Parameters, Camera Stability, 3D Modeling.

SUMMARY

Increasing resolution and lower costs of off-the-shelf digital cameras are giving rise to their utilization in traditional and new photogrammetric activities, such as transportation, surveillance, archaeological, industrial, and medical applications. This progress is allowing amateur users to generate high-quality photogrammetric products using such cameras. For most, if not all photogrammetric applications, the internal metric characteristics, usually known as the Interior Orientation Parameters – IOP, of the implemented camera need to be determined and analyzed. The derivation of these parameters is usually achieved by implementing a bundle adjustment with self-calibration procedure.

The issue of camera stability has been rarely addressed when dealing with analog metric cameras since they have been carefully designed and built to assure the utmost stability of their internal characteristics. However, the stability of digital cameras needs to be investigated since these cameras are not built with photogrammetric applications in mind. This paper introduces three quantitative methods for testing camera stability, where the degree of similarity between reconstructed bundles from two sets of IOP is evaluated. One method assumes that the image coordinate systems associated with the two reconstructed bundles are parallel and that they share the same perspective center. The second method allows the two bundles to rotate relative to each other until the best coincidence is achieved, and the third method allows both spatial and rotational offsets between the two bundles while observing their quality of fit at a given object space.

In this research, the stability of five amateur and professional digital cameras has been checked over a period of thirteen months. The experimental results demonstrate the stability of the majority of these cameras. Some potential applications involving the generation of 3D CAD models, measurement of facial features and medical imaging, will also be discussed in the context of their need for camera calibration and stability analysis.

TS 43 – Deformation Measurement and Analysis   1/17
Ayman Habib, Anoop Pullivelli and Chang-Hahk Hahm
TS43.10 Standardized Measures for the Stability Analysis of Low-Cost Digital Cameras and Potential
Applications

From Pharaohs to Geoinformatics
FIG Working Week 2005 and GSDI-8
Cairo, Egypt April 16-21, 2005

Standardized Measures for the Stability Analysis of Low-Cost Digital Cameras and Potential Applications

Ayman HABIB, Anoop PULLIVELLI and Chang-Hahk HAHM, Canada

1. INTRODUCTION

The primary objective of photogrammetry is to generate three-dimensional spatial and descriptive information from two-dimensional imagery. Reliable and accurate recovery of three-dimensional information from imaging systems requires accurate knowledge of the internal characteristics of the involved camera, which are customarily known as the Interior Orientation Parameters (IOP). To determine the IOP, a bundle adjustment with self-calibration is the commonly employed technique. The calibration procedure requires control information, which is usually available in the form of a test field. Traditional calibration test fields consist of distinct and specifically marked targets (Fryer, 1996). Alternatively, other techniques have been developed for camera calibration using a test field comprised of linear features (Brown, 1971; Chen and Tsai, 1990; Guoqing et al, 1998; Prescott and McLean, 1997; Heuvel, 1999; Bräuer-Burchardt and Voss, 2001; Habib et al, 2002; Habib and Morgan, 2003). The utilization of linear features for camera calibration offers several advantages including: 1) ease of establishing the calibration test field, 2) possibility of automatically extracting the linear features from digital imagery, 3) capability of deriving the distortions associated with the implemented camera by observing deviations from straightness in the captured imagery of object space straight lines (Habib and Morgan, 2003).

Since its inception, the use of film/analog metric cameras has been the norm in photogrammetric applications. However, the role of digital cameras in such applications has been rising along with its rapid development, ease of use, and availability. Analog metric cameras, which are solely designed for photogrammetric applications, proved to possess a strong structural relationship between the elements of the lens system and the focal plane. Practical experience with these cameras showed that they maintain the stability of their IOP over an extended period of time. On the other hand, the majority of commercially available digital cameras are not designed with photogrammetric applications in mind. Therefore, the stability of their internal characteristics should be carefully examined prior to their use in photogrammetric applications. To analyze camera stability, a few methodologies for comparing two sets of IOP of the same camera that have been derived from two calibration sessions will be presented. The objective of the presented methodologies is to decide whether the two IOP sets are equivalent or not. It should be noted that these methodologies are general enough that they are applicable for stability analysis of analog and digital cameras.

The paper will first start with a concise background about camera calibration. This will be followed by a detailed explanation of the developed methodologies for checking camera stability. The experimentation results from the stability analysis tests will be given in section 4. Then a description of some potential applications involving camera calibration and

stability will be presented in section 5. Finally, section 6 will conclude with a brief summary and recommendations for future work.

2. CALIBRATION

The purpose of camera calibration is to determine numerical estimates of the IOP of the implemented camera. The IOP comprises the principal distance (c), location of the principal point (x_p, y_p), and image coordinate corrections that compensate for various deviations from the assumed perspective geometry. The assumed perspective geometry is described by the collinearity condition, which states that the perspective center, the object point, and the corresponding image point must be collinear. Such a condition is mathematically defined by Equations 1.

$$x_a = x_p - c\frac{r_{11}(X_A - X_O) + r_{21}(Y_A - Y_O) + r_{31}(Z_A - Z_O)}{r_{13}(X_A - X_O) + r_{23}(Y_A - Y_O) + r_{33}(Z_A - Z_O)} + \Delta x$$

$$y_a = y_p - c\frac{r_{12}(X_A - X_O) + r_{22}(Y_A - Y_O) + r_{32}(Z_A - Z_O)}{r_{13}(X_A - X_O) + r_{23}(Y_A - Y_O) + r_{33}(Z_A - Z_O)} + \Delta y \tag{1}$$

Where:

x_a and y_a are the image coordinates,
X_A, Y_A and Z_A are the corresponding ground coordinates,
Δx and Δy are the compensations for deviations from the collinearity condition,
x_p, y_p and c are the principal point coordinates and principal distance,
X_O, Y_O, Z_O are the ground coordinates of the exposure station (perspective center), and
r_{11}, r_{12}…, r_{33} are the elements of a rotation matrix describing the attitude of that image.

In order to determine the IOP of the camera, a bundle adjustment with self-calibration procedure is carried out with the use of control information in the form of a test field. In a traditional calibration test field, numerous control points are precisely surveyed prior to the calibration process. Establishing a traditional calibration test field is not a trivial task and it requires professional surveyors. Therefore, an alternative approach for camera calibration using an easy-to-establish test field comprised of a group of straight lines is implemented in this research (Habib et al, 2002; Habib and Morgan, 2003). Once the calibration procedure has been carried out, the IOP of the camera that are derived from two different calibration sessions should be inspected to test its stability.

3. STABILITY ANALYSIS

The desired outcome of stability analysis is to determine whether two sets of IOP are equivalent to each other. Shortis et al. (2001) described a method for evaluating digital camera stability by using the ratio of the mean precision of target coordinates to the largest dimension of the target array. However, to the best of the authors' knowledge, there has not been a comprehensive study to quantify and introduce meaningful measures for the stability

TS 43 – Deformation Measurement and Analysis
Ayman Habib, Anoop Pullivelli and Chang-Hahk Hahm
TS43.10 Standardized Measures for the Stability Analysis of Low-Cost Digital Cameras and Potential Applications

3/17

of the IOP of digital cameras for photogrammetric applications. This void in the literature can be attributed to the absence of standards for quantitative analysis of camera stability.

The ultimate objective of camera calibration is to derive a bundle of light rays (as defined by the IOP and points along the image plane), which is as similar as possible to the incident bundle onto the camera at the moment of exposure. Therefore, camera stability should be checked by quantitatively estimating the degree of similarity between reconstructed bundles from two sets of IOP. In this research, three meaningful methods for evaluating the similarity between two IOP sets derived from two calibration sessions are introduced and described in the following sections.

3.1 Zero Rotation (ZROT) Method

A bundle of light rays is typically defined by the IOP of the camera together with points along the image plane. The analysis for stability using the Zero Rotation (ZROT) method can be initiated by defining a bundle of light rays for each of the two sets of IOP that are being tested for similarity. The two bundles will share the same perspective center and have parallel image coordinate systems, Figure 1. To create the two bundles, the procedure starts off by first defining a synthetic regular grid in the two-dimensional image plane. This is followed by removing various distortions at the defined grid vertices using the two IOP sets that are being compared. The result will be the creation of two distortion-free points for each grid point.
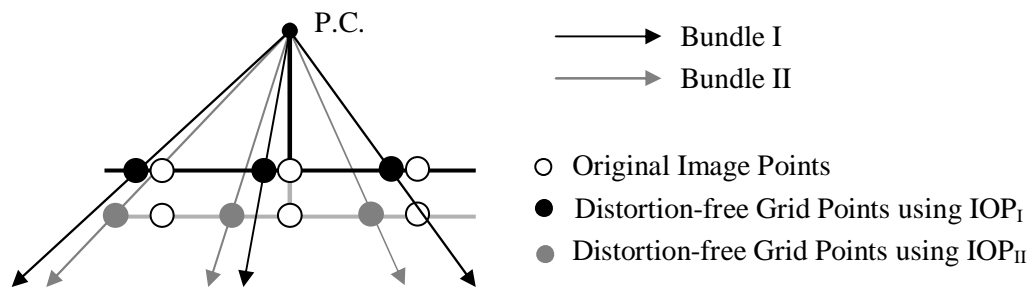

Figure 1 – Two bundles of light rays with same perspective center and parallel image coordinate systems defined by two sets of IOP

To estimate the offset between the two IOP sets, the x and y coordinate difference between the two distortion-free points of each grid point is computed. However, the two distortion-free points may not necessarily be on the same plane since the principal distance of the two IOP sets could be different. Hence, the distortion-free grid points of one IOP set have to be projected onto the image plane of the other IOP set. This is accomplished by the formulas provided in Equations 4, where (x_2, y_2) are the distortion-free coordinates of a grid point according to the second IOP set, (x'_2, y'_2) are the same coordinates projected onto the image plane of the first IOP set, and c_1 and c_2 are the principal distances of the first and second IOP set, respectively.

TS 43 – Deformation Measurement and Analysis   4/17
Ayman Habib, Anoop Pullivelli and Chang-Hahk Hahm
TS43.10 Standardized Measures for the Stability Analysis of Low-Cost Digital Cameras and Potential
Applications

From Pharaohs to Geoinformatics
FIG Working Week 2005 and GSDI-8
Cairo, Egypt April 16-21, 2005

$$x'_2 = x_2 \frac{c_1}{c_2} \; ; \qquad y'_2 = y_2 \frac{c_1}{c_2} \qquad\qquad (4)$$

Once all the points are on the same plane, the offset (i.e. the x and y coordinate differences) between the two distortion-free points of each grid point is computed, Figure 2. The degree of similarity is given by the root mean square error (RMSE) of these computed offsets. If the RMSE is within the range defined by the expected standard deviation of the image coordinate measurements, the two sets of IOP are considered similar.
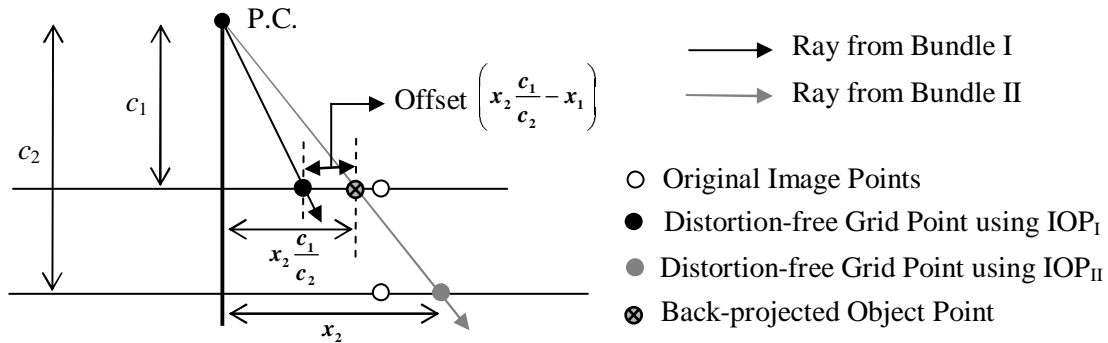

Figure 2 – The offset between distortion-free coordinates in the Zero Rotation method

3.2 Rotation (ROT) Method

The ZROT method of comparison assumes the coincidence of the optical axes of the reconstructed bundles defined by the two IOP sets. However, stability analysis should be concerned with determining whether conjugate light rays coincide with each other regardless of the orientation of the respective image coordinate systems. Therefore, one has to check if there is a unique set of rotation angles (ω, φ, κ) that can be applied to the first bundle to produce the second one while maintaining the same perspective center, Figure 3.
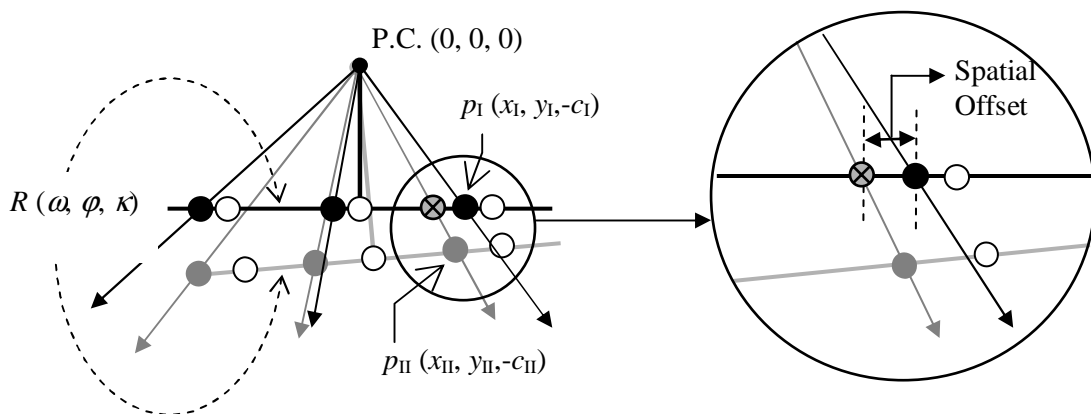

Figure 3 – The two bundles in the ROT method are rotated to reduce the angular offset between conjugate light rays

As shown in Figure 3, $(x_I, y_I, -c_I)$ and $(x_{II}, y_{II}, -c_{II})$ are the three-dimensional vectors connecting the perspective center and the distortion-free coordinates of the same image point according to IOP_I and IOP_{II}, respectively. To make the two vectors coincide with each other, the first vector has to be rotated until it is aligned along the second vector. The coincidence of the two vectors after applying the rotation angles can be mathematically expressed by Equation 5.

$$\begin{bmatrix} x_I \\ y_I \\ -c_I \end{bmatrix} = \lambda \ R^T(\omega, \phi, \kappa) \begin{bmatrix} x_{II} \\ y_{II} \\ -c_{II} \end{bmatrix} \tag{5}$$

To eliminate the scale factor (λ), the first two rows in Equation 5 are divided by the third one producing Equations 6.

$$x_I = -c_I \ \frac{r_{11} \ x_{II} + r_{21} \ y_{II} - r_{31} \ c_{II}}{r_{13} \ x_{II} + r_{23} \ y_{II} - r_{33} \ c_{II}}$$

$$y_I = -c_I \ \frac{r_{12} \ x_{II} + r_{22} \ y_{II} - r_{32} \ c_{II}}{r_{13} \ x_{II} + r_{23} \ y_{II} - r_{33} \ c_{II}} \tag{6}$$

Equations 6 represent the necessary constraints for making the two bundles defined by IOP_I and IOP_{II} coincide with each other as well as possible. Having (n) conjugate points, one can produce (2n) constraints of the form in Equations 6. These constraints can be used to solve for the rotation angles (ω, φ, κ) using a least-squares adjustment. The variance component (σ_o^2), which is the variance of an observation of unit weight, resulting from the adjustment procedure represents the quality of the coincidence between the two bundles after applying the estimated rotation angles. The smaller the variance component, the more similar the two bundles are to each other. A closer investigation of the estimated residuals from Equations 5 would reveal a more meaningful clue regarding the value of the estimated variance component (σ_o^2).

Assuming that (x_I, y_I) in Equations 6 are the observed values, the corresponding residuals represent the spatial offset between the two bundles, after applying the rotation angles, along the image plane defined by the first IOP set, Figure 3. Therefore, assigning a unit weight to all the constraints resulting from various image points yields a variance component that represents the variance of the spatial offset between the two bundles along the image plane. A relative comparison between the computed variance component and the expected variance of image coordinate measurements would reveal whether the two bundles are significantly different from each other or not. The evaluation of the degree of similarity between the two bundles can be summarized as follows:

i. Define a synthetic regular grid in the image plane.
ii. Remove various distortions at the defined grid vertices using the derived IOP from two calibration sessions.

TS 43 – Deformation Measurement and Analysis   6/17
Ayman Habib, Anoop Pullivelli and Chang-Hahk Hahm
TS43.10 Standardized Measures for the Stability Analysis of Low-Cost Digital Cameras and Potential
Applications

From Pharaohs to Geoinformatics
FIG Working Week 2005 and GSDI-8
Cairo, Egypt April 16-21, 2005

iii. Define two bundles of light rays using the principal distance, principal point coordinates, and distortion-free coordinates of the grid vertices.
iv. Assuming the same perspective centre, derive an estimate of the rotation angles (ω, φ, κ) that are needed to make the two bundles coincide with each other as well as possible according to the constraints in Equations 6.
v. Compare the estimated variance component (σ_o^2), resulting from the adjustment procedure in the previous step, to the expected variance of the image coordinate measurements. If the variance component is within the range defined by the variance of the image coordinate measurement, the two IOP sets are deemed to be similar.

The ROT method provides a meaningful measure for evaluating the degree of similarity between two bundles of light rays, defined by two sets of IOP, sharing the same origin (perspective center) regardless of their orientation in space. However, it is possible that the IOP and the positional component of the EOP (X_O, Y_O, Z_O in Equations 1) are correlated. Therefore another methodology has been developed to compare the two bundles while allowing for rotational and spatial offsets between them to compensate for such correlations. This can be achieved through an object space comparison by observing the fit between the defined bundles at a given object space.

3.3 Single Photo Resection (SPR) Method

In contrast to the ROT method, the SPR method evaluates the quality of fit between the two bundles at a given object space while allowing for spatial and rotational offsets between the respective image coordinate systems. In other words, the two bundles are permitted to have different perspective centers. The methodology for evaluating the degree of similarity between the two bundles in terms of their fit at a given object space can proceed as follows:
 i. Define a regular grid in the image plane.
 ii. Use the available IOP sets to derive two sets of distortion-free coordinates of the grid vertices.
iii. Define a bundle of light rays for the first IOP set using the perspective center together with the corresponding distortion-free grid vertices.
iv. Intersect the defined bundle with an arbitrary object space to produce a set of object points, as shown in Figure 4.
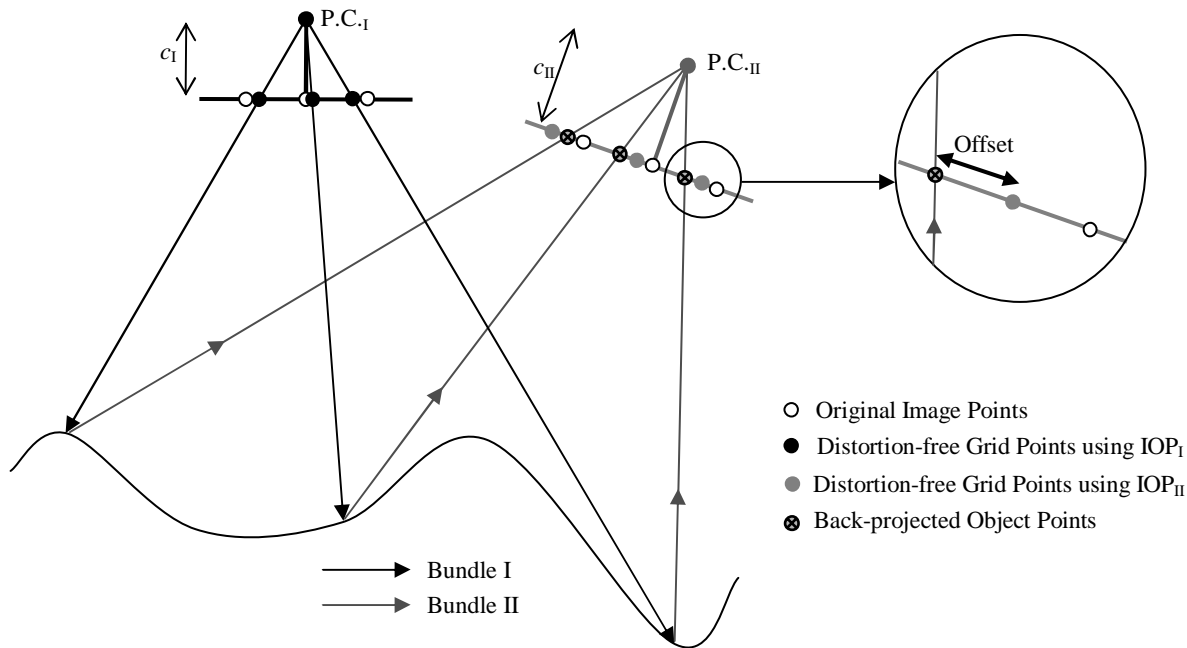
Figure 4 – SPR method allows for spatial and rotational offsets between the two bundles to achieve the best fit at a given object space

v. Use the derived object points and the corresponding distortion-free grid vertices, according to the second set of IOP, in a Single Photo Resection (SPR) procedure to estimate the position and the attitude of the second bundle that fits the object space as defined by the given set of object points.

vi. The variance component resulting from the SPR procedure represents the variance of the spatial offset between the distortion-free grid vertices that are defined by the second set of IOP, and the computed image coordinates from back projecting the object points onto the respective image plane, Figure 4.

Similar to the ZROT and ROT methodologies, if the estimated variance component lies within the range defined by the expected variance of image coordinate measurements, the two bundles are deemed to have a good fit at the given object space. It is expected that the SPR method with a relatively flat object space will lead to a good fit between the two bundles at the object space, even if the two IOP sets are significantly different from each other. This will be the case since the estimated EOP will adapt (shift and rotate) in a way to absorb the differences between the involved IOP. The ZROT method on the other hand, is expected to give conservative results since the position and orientation of the bundles are fixed.

4. EXPERIMENTAL RESULTS

In this research, a few cameras were calibrated and checked for stability using the introduced methodologies over an extended period of time. A two-dimensional test field consisting of straight lines and points was used for the calibration procedure, Figure 5. Straight lines and

TS 43 – Deformation Measurement and Analysis
Ayman Habib, Anoop Pullivelli and Chang-Hahk Hahm
TS43.10 Standardized Measures for the Stability Analysis of Low-Cost Digital Cameras and Potential Applications

From Pharaohs to Geoinformatics
FIG Working Week 2005 and GSDI-8
Cairo, Egypt April 16-21, 2005

8/17

distinct points were established on a 3.5 x 7.0 meter section of a white wall. The lines were thin, dark ropes that were stretched between nails on the wall. For each calibration session, eighteen converging and overlapping images were captured at locations that were roughly four to five meters away from the closest point on the test field. The calibration procedure was carried out according to the methodology explained in (Habib and Morgan, 2003). Five digital cameras, ranging in price from $500 to $6000, have been calibrated and checked for stability. They are all Single-lens Reflex (SLR) cameras with Charged-coupled Device (CCD) sensors. Table 1 summarizes the characteristics of the implemented cameras along with the designated names of each.

Table 1 – Characteristics of implemented cameras

Camera (Names Designated in experiments)	Price Range ($ US)	Max. Output Resolution (pixels)	Pixel Size (mm/pixel)	Effective Pixels (Mega Pixels)
Canon EOS 1D (Canon1 and Canon2)	$5000	2464x1648	0.0115	4.15
Nikon 4500 (Nikon)	$500 - $600	2272x1704	0.0031	3.87
Rollei d 7 metric (Rollei)	$6000	2552x1920	0.004	4.90
Sony DSC-F707 (Sony)	$650 - $800	2560x1920	0.004	4.92

The above digital cameras were calibrated and evaluated for their stability over a thirteen-month period. For each camera, image datasets were acquired in three or more months. As mentioned in section 3, the spatial offset between two bundles obtained from two sets of IOP is given by the RMSE in the ZROT method and by the square root of the variance component (σ_o) in the ROT and SPR methods. If these values (RMSE or σ_o) are not significantly larger than the expected image coordinate measurement accuracy, which can be considered to be approximately one-half to two-thirds of a pixel, then the two sets of IOP are deemed similar.

The stability analysis results for the five digital cameras (denoted by their experiment names) are listed in Tables 2 - 7. These results are derived using all three methods of comparison. Based on the reported numbers in Tables 2-5, one can see that all the tested cameras are stable according to the ROT and SPR methods. As mentioned in section 3.3, the ZROT method is expected to give conservative results. Hence, all the cameras fail the stability test under the ZROT method even though they are considered similar under the other two methods. Based on the results in Table 6, the Nikon camera is the only one that did not show good long-term stability according to the ZROT and ROT methods. However, it did show good stability according to the SPR method, but this is deceiving since SPR provides a very relaxed degree of similarity. Hence, further experiments were conducted to see whether this camera had good short-term stability (i.e. comparing sets that were acquired on the same day by switching the camera off and on between dataset acquisitions). The majority of the results in Table 7 indicate that the Nikon does not maintain the same IOP values according to the ZROT and ROT methods, even in a short time period, and is considered unstable.

TS 43 – Deformation Measurement and Analysis   9/17
Ayman Habib, Anoop Pullivelli and Chang-Hahk Hahm
TS43.10 Standardized Measures for the Stability Analysis of Low-Cost Digital Cameras and Potential Applications

From Pharaohs to Geoinformatics
FIG Working Week 2005 and GSDI-8
Cairo, Egypt April 16-21, 2005

Table 2 Stability comparison of IOP sets for Canon1 (RMSE or $\sigma_o < 0.0077$ → IOP sets similar)

ID	Date		ZROT		ROT		SPR	
	IOP Set I	IOP Set II	RMSE (mm)	Similar	σ_o (mm)	Similar	σ_o (mm)	Similar
1	Jul 03	Oct 03	0.02213	No	0.00256	Yes	0.00196	Yes
2	Jul 03	Aug 04	0.03130	No	0.00236	Yes	0.00171	Yes
3	Oct 03	Aug 04	0.03777	No	0.00202	Yes	0.00176	Yes

Table 3 – Stability comparison of IOP sets for Canon2 (RMSE or $\sigma_o < 0.0077$ → IOP sets similar)

ID	Date		ZROT		ROT		SPR	
	IOP Set I	IOP Set II	RMSE (mm)	Similar	σ_o (mm)	Similar	σ_o (mm)	Similar
1	Jul 03	Oct 03	0.03934	No	0.00293	Yes	0.00266	Yes
2	Jul 03	Aug 04	0.04606	No	0.00466	Yes	0.00289	Yes
3	Oct 03	Aug 04	0.01009	No	0.00356	Yes	0.00062	Yes

Table 4 – Stability comparison of IOP sets for Rollei (RMSE or $\sigma_o < 0.003$ → IOP sets similar)

ID	Date		ZROT		ROT		SPR	
	IOP Set I	IOP Set II	RMSE (mm)	Similar	σ_o (mm)	Similar	σ_o (mm)	Similar
1	Jul 03	Oct 03	0.02681	No	0.00290	Yes	0.00156	Yes
2	Jul 03	Jan 04	0.01569	No	0.00147	Yes	0.00092	Yes
3	Oct 03	Jan 04	0.01430	No	0.00146	Yes	0.00092	Yes
4	Jul 03	Aug 04	0.01811	No	0.00197	Yes	0.00119	Yes
5	Oct 03	Aug 04	0.01108	No	0.00116	Yes	0.00092	Yes
6	Jan 04	Aug 04	0.00329	No	0.00060	Yes	0.00039	Yes

Table 5 – Stability comparison of IOP sets for SonyF707 (RMSE or $\sigma_o < 0.003$ → IOP sets similar)

ID	Date		ZROT		ROT		SPR	
	IOP Set I	IOP Set II	RMSE (mm)	Similar	σ_o (mm)	Similar	σ_o (mm)	Similar
1	Jul 03	Oct 03	0.01800	No	0.00206	Yes	0.00106	Yes
2	Jul 03	Feb 04	0.01877	No	0.00176	Yes	0.00109	Yes
3	Oct 03	Feb 04	0.00349	No	0.00291	Yes	0.00031	Yes
4	Jul 03	Oct 04	0.02392	No	0.00167	Yes	0.00106	Yes
5	Oct 03	Oct 04	0.00680	No	0.00280	Yes	0.00039	Yes
6	Feb 04	Oct 04	0.00543	No	0.00031	Yes	0.00028	Yes

Table 6 – Long-term stability comparison for Nikon (RMSE or $\sigma_o < 0.0021$ → IOP sets similar)

ID	Date		ZROT		ROT		SPR	
	IOP Set I	IOP Set II	RMSE (mm)	Similar	σ_o (mm)	Similar	σ_o (mm)	Similar
1	Jan 04	Aug 04	0.00674	No	0.00566	No	0.00062	Yes
2	Jan 04	Oct 04	0.00299	No	0.00285	No	0.00031	Yes
3	Aug 04	Oct 04	0.00480	No	0.00280	No	0.00032	Yes

Table 7 – Short-term stability comparison for Nikon (RMSE or σ_o < 0.0021 → IOP sets similar)

ID	Date		ZROT		ROT		SPR	
	IOP Set I	IOP Set II	RMSE (mm)	Similar	σ_o (mm)	Similar	σ_o (mm)	Similar
1	Jan 04 / Set 1	Jan 04 / Set 2	0.00804	No	0.00618	No	0.00067	Yes
2	Aug 04 / Set 1	Aug 04 / Set 2	0.11815	No	0.05533	No	0.00699	No
3	Oct 04 / Set 1	Oct 04 / Set 2	0.00254	No	0.00061	Yes	0.00009	Yes

5. APPLICATIONS

Low-cost digital cameras can be implemented in a number of diverse applications with respect to the generation of three-dimensional information. The applications investigated in this research include the measurement of facial features for personal identification, the generation of 3-D CAD models of buildings for archiving, and the reconstruction of a human torso for modeling spinal disorders. The procedures involved in these potential applications will be discussed in the following sections.

5.1 Facial Measurements

The measurement of facial features on a human face is a task that could be useful for video surveillance at banks, stores or other potential areas where identification of a person is required. The core objective of making facial measurements is to identify the person by the geometry of the face. The process starts by capturing images, a left and a right image, of the person (subject). Using the acquired images, the outside corners of each subject's eyes and the top central position of the subject's lip are measured to establish a triangle on the face. The area of this triangle can be computed as a basis for identification. The measurement of the vertices of the triangle needed to calculate the area of the face can be seen in Figure 5.
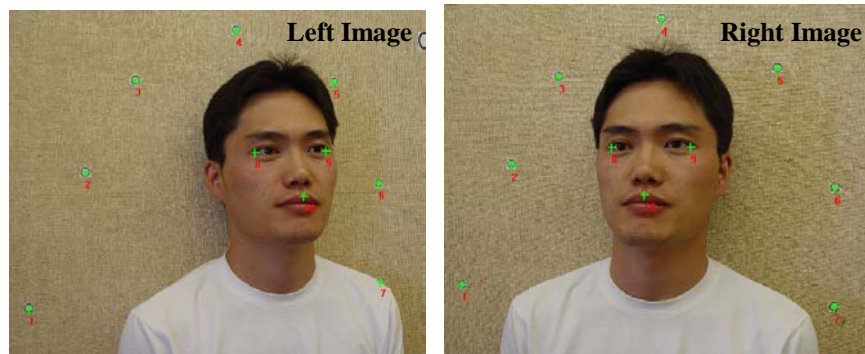

Figure 5 – Left and right images showing the configuration of the facial measurements

After making the measurements of points on the face and control points in the image, the three-dimensional coordinates of the three points are recovered in an intersection procedure. Using the computed coordinates, the area occupied by joining these points is then calculated.

In these experiments, there were four sets of a stereo image pair taken of four subjects. Four image sets were captured for each subject to prove that the measurements are repeatable and consistent. For each of the four datasets of each subject, a facial area was computed as well as the average and standard deviation of the four area values. The standard deviation represents the discrepancy between the measurements made from an image capture of a subject at one time and those of a later time. The results of these computations can be seen in Table 8. When looking at the four areas computed for each subject, it is evident that all values are fairly close to each other. The standard deviations show that it is possible to determine a facial area with any dataset (i.e. a dataset acquired at any time). Therefore, once a facial area has been determined and recorded from one dataset, a match can be made to an area computed from a later dataset capture to identify the person with relatively good accuracy. This application could explore numerous avenues of enhancements by incorporating a combination of distances, areas and volumes to identify the person. Furthermore, the automation of facial feature measurements could be investigated.

Table 8 – Computed facial areas with each subject's average area and standard deviations

Subject	Area (cm^2)					
	Dataset 1	Dataset 2	Dataset 3	Dataset 4	Average	Standard Deviation
Subject 1	29.28	29.50	28.87	29.25	29.22	0.26
Subject 2	26.98	26.78	26.88	26.55	26.80	0.18
Subject 3	34.57	34.93	34.28	35.06	34.71	0.35
Subject 4	38.09	37.52	37.16	37.75	37.63	0.39

5.2 3-D CAD Model Generation

Utilizing imagery to generate three-dimensional CAD models is useful in a wide variety of applications such as architecture, archaeology, building inspections, and archiving of historical sites (Habib et al, 2004). This research investigates the use of a low-cost digital camera to create a three-dimensional model of a building. The first step is to capture convergent and overlapping imagery around the building, Figure 6 (a). Using the acquired images, measurements of carefully selected points on the building are made. It is crucial that an adequate number of points are selected for the reconstruction of the building. These point measurements are then introduced into the bundle adjustment process in order to estimate their ground coordinates. In the adjustment, an arbitrary datum is chosen as reference for the object space and the scale is established by incorporating a few measured distances. The accuracy of the derived point coordinates from the adjustment is tested by computing the distance between them and comparing these distances with the ones measured in the field. It was found that there was approximately a 1-4 mm difference between the computed and measured distances.

Once coordinates of the points are computed, they are then imported into a CAD modeling program like AutoCAD where a wire-frame model of the building can be created. From this wire-frame representation, a rendered surface is generated with real-world surface texture by

adding material and lighting provided by AutoCAD, Figure 6 (b). This modeling method is reliable and has varying degrees of flexibility with respect to the level of detail.
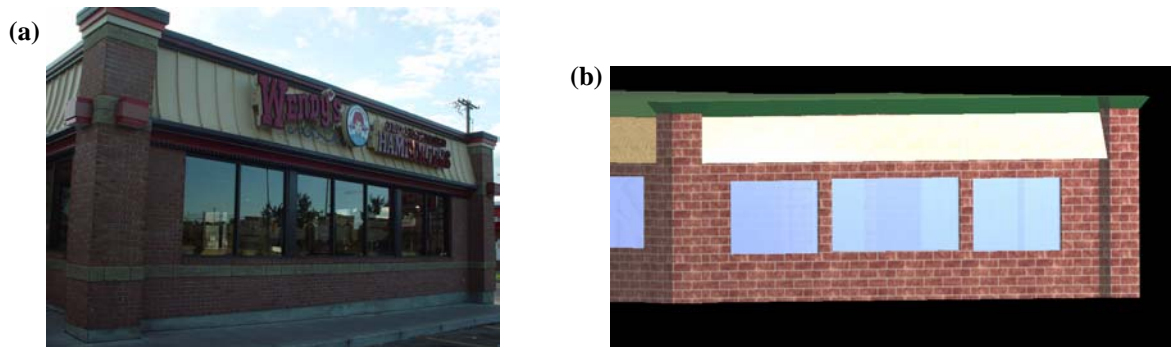

Figure 6 – A real image (a) and a reconstructed 3-D CAD image (b) of a building

5.3 Medical Imaging

Photogrammetric techniques are commonly and increasingly being used in the modeling and reconstruction of body parts like spines, rib cages and bones. One such application involves a three-dimensional reconstruction of an artificial scoliotic human torso that is used to help analyze and treat a spinal deformity called scoliosis. In the work of (Robu et al, 2004), a Coordinate Measuring Machine (CMM) is utilized to measure markers on the torso to derive three-dimensional positions of these targets. A CMM is a high-end measuring system designed to move a measuring probe to determine coordinates of points on an object with very high precision and accuracy. In the experiments conducted in this research, photogrammetric methods are used to measure and determine coordinates of the targets on the torso and compare these derived coordinates to those determined by the CMM. There were two cameras utilized in the experiments, a Sony F707 and a Rollei. One set of images were captured using the Sony F707 and two sets of images were captured using the Rollei. For each image set, approximately sixteen overlapping images are captured at locations surrounding the torso. To establish the datum, some nearby points in the area that are not on the torso are arbitrarily fixed. These fixed points, the target points on the torso, and tie points in the surrounding area are then measured in the imagery, Figure 7.

After the measurements are carried out, the coordinates of the targets can be derived in a reconstruction procedure. The accuracy of the measurements is represented by the variance component (σ_o) obtained in the adjustment. In these experiments, two operators measure the targets to confirm the repeatability and consistency of the measurements. The derived coordinates are then used to compute distances between them and these distances are compared to those obtained by the CMM coordinate measurements. To compare the two measurement techniques, the root mean square error of the differences between the photogrammetric and CMM distances are computed. These distance differences as well as the measurement accuracies are presented in Table 9. These results show that there is approximately only a 1.0 mm difference between the distances and signify that

photogrammetric techniques can attain accuracies that are comparable to those achieved by sophisticated devices like the CMM.
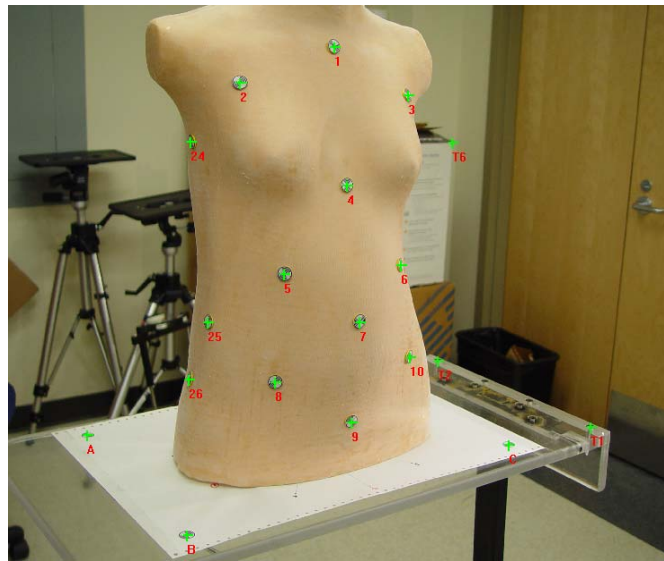

Figure 7 – Measurement of targets on an artificial human torso and tie points in the surrounding area

Table 9 – Torso measurement accuracy and comparison with CMM measurements

Dataset	Operator	σ_o (mm)	Distance comparison with CMM – RMSE (mm)
SonyF707 – Set 1	Operator 1	2.55e-003	0.943
	Operator 2	2.51e-003	1.017
Rollei – Set 1	Operator 1	2.65e-003	1.002
	Operator 2	2.58e-003	0.915
Rollei – Set 2	Operator 1	3.28e-003	1.134
	Operator 2	4.84e-003	1.125

6. CONCLUSION

The presented research outlined three new methodologies for evaluating the stability of off-the-shelf digital cameras. These methodologies are based on evaluating the degree of similarity between reconstructed bundles defined by two sets of IOP, which are derived from two calibration sessions. Each method imposes constraints regarding the position and attitude of the defined bundles in space. In the ZROT method, the two bundles are fixed in the same position and orientation and hence, it provides a very strict measure of similarity. The ROT method allows the bundles to rotate and therefore, is not as conservative as the ZROT method. The SPR method, however, allows the bundles to both shift and rotate and hence, provides the most relaxed measure of similarity. It should be noted that these stability measures are general enough that they can be applied to digital as well as analog cameras intended for mapping applications. These measures would allow amateur users of digital

TS 43 – Deformation Measurement and Analysis
Ayman Habib, Anoop Pullivelli and Chang-Hahk Hahm
TS43.10 Standardized Measures for the Stability Analysis of Low-Cost Digital Cameras and Potential Applications

From Pharaohs to Geoinformatics
FIG Working Week 2005 and GSDI-8
Cairo, Egypt April 16-21, 2005

cameras to evaluate their stability. In addition, the developed measures do not require additional field work to evaluate camera stability and the statistical properties of the available IOP sets are not needed.

There were five amateur and professional digital cameras tested in the experiments. The experimental analysis of the cameras revealed that the IOP remained stable over a thirteen-month period for most of these cameras. The only exception was the stability of the Nikon cameras, which showed poor long-term as well as short-term stability. Applications involving the measurement of facial features, the three-dimensional reconstruction of a building for archiving and the modeling of a torso for medical treatments demonstrated the usefulness of the presented calibration and stability analysis techniques. Current research is focused on the implication of direct and indirect geo-referencing techniques on the stability requirement of digital cameras. Since the three stability measures have varying degrees of strictness, a specific stability method can be applied depending on the constraints introduced by the implemented geo-referencing technique.

ACKNOWLEDGEMENT

REFERENCES

1. Bräuer-Burchardt C. and Voss K. (2001), "A new algorithm to correct fish-eye and strong wide-angle-lens-distortion from single images", Proceedings of the 2001 International Conference on Image Processing, October 7-10, 2001, Thessaloniki, Greece, Volume 1, pp. 225-228.
2. Brown D. (1971), "Close range camera calibration", Journal of Photogrammetric Engineering & Remote Sensing, 37 (8): 855-866.
3. Chen S., and Tsai W. (1990), "A systematic approach to analytic determination of camera parameters by line features", Pattern Recognition, 23(8): 859-877.
4. Fryer J. (1996), "Camera calibration", Close range Photogrammetry and machine vision, (K.B. Atkinson, editor), Whittles Publishing, Caithness, Scotland, pp. 156-180.
5. Guoqing Z., Ethrog U., Wenhao F., and Baozong Y. (1998), "CCD camera calibration based on natural landmarks", Pattern Recognition, 31(11): 1715-1724.
6. Habib A., Morgan M., and Lee Y. (2002), "Bundle Adjustment with Self-Calibration using Straight Lines", Journal of Photogrammetric Record, 17(100): 635-650.
7. Habib A., and Morgan M. (2003), "Automatic Calibration of Low Cost Digital Cameras", SPIE Journal of Optical Engineering, 42(4): 948-955.

TS 43 – Deformation Measurement and Analysis   15/17
Ayman Habib, Anoop Pullivelli and Chang-Hahk Hahm
TS43.10 Standardized Measures for the Stability Analysis of Low-Cost Digital Cameras and Potential
Applications

From Pharaohs to Geoinformatics
FIG Working Week 2005 and GSDI-8
Cairo, Egypt April 16-21, 2005

8. Habib A., Ghanma M., Al-Ruzouq R., and Kim E. (2004), 3-D Modeling of Historical Sites Using Low-Cost Digital Cameras, XXth ISPRS Congress, Istanbul, Turkey, Commission 5, SS4-CIPA-Low-Cost Systems in Recording and Managing the Cultural Heritage, pp.570.

9. Heuvel F. (1999), "Estimation of interior orientation parameters from constraints on line measurements in a single image", Proceedings of International Archives of Photogrammetry and Remote Sensing, Thessaloniki, Greece, 7-9 July, 32 (5W11): 81-88.

10. Koch K. (1999), "Parameter Estimation and Hypothesis Testing in Linear Models", Second Edition, Springer-Verlag, Berlin, Heidelberg, 333p.

11. Prescott B., and McLean G. (1997), "Line-Based Correction of Radial Lens Distortion", Graphical Models and Image Processing, 59(1): 39-47.

12. Robu D., Poncet P., Zernicke R., Ronsky J. (2004), "Assessment of 3D Reconstruction of Scoliotic Human Torso using Imaging Techniques and Stereo-Radiography", GEOIDE 6th Annual Scientific Conference, Hull, Quebec, poster presentation.

13. Shortis M., Ogleby C., Robson S., Karalis E., and Beyer H. (2001), "Calibration Modeling and Stability Testing for the Kodak DC200 Series Digital Still Camera", Proceedings of SPIE on Videometrics and Optical Methods for 3D Shape Measurements, San Jose, CA, 22-23 January 2001, Volume 4309, pp. 148-153.

BIOGRAPHICAL NOTES

Ayman F. Habib received an MSc in civil engineering from Cairo University, Egypt, an MSc and a PhD in Photogrammetry from the Ohio State University, USA. Currently, he is an associate professor at the Department of Geomatics Engineering, University of Calgary, Canada. His research interests span the fields of terrestrial and aerial mobile mapping systems, modeling the perspective geometry of imaging scanners, automatic matching and change detection, incorporation of linear features in various orientation procedures, object recognition in imagery, and integration of photogrammetric data with other sensors/datasets.

Anoop M. Pullivelli received a BSc in Geomatics engineering from the University of Calgary. At present, he is a research and teaching assistant and is working towards an MSc degree at the same university. His current research interests include automatic calibration and stability analysis of low-cost digital cameras.

Chang-Hahk Hahm received an MSc in civil engineering from Inha University, Korea, and a PhD in civil engineering from Chungbuk National University, Korea. Currently, he is a professor in the Department of Aerial Geoinformatics at Inha Technical College where his research interests include photogrammetry, GIS and surveying.

TS 43 – Deformation Measurement and Analysis
Ayman Habib, Anoop Pullivelli and Chang-Hahk Hahm
TS43.10 Standardized Measures for the Stability Analysis of Low-Cost Digital Cameras and Potential Applications

16/17

From Pharaohs to Geoinformatics
FIG Working Week 2005 and GSDI-8
Cairo, Egypt April 16-21, 2005

CONTACTS

Dr. Ayman Habib (Associate Professor), Mr. Anoop Pullivelli (Graduate Research Associate), Dr. Chang-Hahk Hahm (Professor)
Department of Geomatics Engineering, University of Calgary
2500 University Drive NW, Calgary, Alberta, T2N 1N4, Canada
Tel: +1 403-220-7105 (Office); 403-284-1980 (Fax)
E-mail: habib@geomatics.ucalgary.ca
Website: http://www.geomatics.ucalgary.ca/~habib/

TS 43 – Deformation Measurement and Analysis   17/17
Ayman Habib, Anoop Pullivelli and Chang-Hahk Hahm
TS43.10 Standardized Measures for the Stability Analysis of Low-Cost Digital Cameras and Potential
Applications

From Pharaohs to Geoinformatics
FIG Working Week 2005 and GSDI-8
Cairo, Egypt April 16-21, 2005